Arch. Metall. Mater. **67** (2022), 1, 197-202

DOI: https://doi.org/10.24425/amm.2022.137489

FONG SUE MIN[1], HEAH CHENG YONG[1,2*], LIEW YUN MING[1,3], MOHD MUSTAFA AL BAKRI ABDULLAH[1,3], HASNIYATI MD RAZI[4], FOO WAH LOW[5], NG HUI-TENG[1,2], NG YONG-SING[1,2]

EFFECT OF SILICA FUME AND ALUMINA ADDITION ON THE MECHANICAL AND MICROSTRUCTURE OF FLY ASH GEOPOLYMER CONCRETE

This paper discussed the effect of the addition of silica fume (2 wt.% and 4 wt.%) and alumina (2 wt.% and 4 wt.%) on the properties of fly ash geopolymer concrete. The fly ash geopolymer concrete achieved the highest 28-day compressive strength with 2 wt.% of silica fume (39 MPa) and 4 wt.% of alumina (41 MPa). The addition of 2 wt.% of silica fume increased the compressive strength by 105% with respect to the reference geopolymer (without additive). On the other hand, the compressive strength surged by 115% with 4 wt.% of alumina compared to the reference geopolymer. The addition of additives improved the compactness of the geopolymer matrix according to the morphology analysis.

Keywords: geopolymer; concrete; silica fume; alumina

1. Introduction

Geopolymer concrete consists of geopolymer binders, coarse and fine aggregates. The geopolymer binder is synthesized by alkali activation of aluminosilicates with an alkaline medium by geopolymerization [1]. The geopolymerization involves the immediate dissolution of Si and Al in alkali medium and polycondensation process to form polymeric chain of Si-O-Al-O bonds with three-dimensional structure followed by solidification process to form a rigid body [2,3].

Additives and reinforcements are commonly incorporated into geopolymer to increase the mechanical performance of geopolymer. Silica fume and alumina could be added into geopolymer concrete as an additional source of Si and Al. It has been proven that the addition of silica and alumina will yield geopolymer with better mechanical strength [4]. For instance, Liu et al. [5] reported excellent compressive strength of 151 MPa for steel-fiber-reinforced fly ash/slag geopolymer added with 30 wt.% of silica fume. Okoye et al. [6] stated that increasing silica fume content from 5 wt.% to 40 wt.% increased the compressive strength of fly ash geopolymer concretes. Nmiri et al. [7] replaced metakaolin precursors with 2 wt.%, 6 wt.% and 10 wt.% of silica fume and achieved the highest compressive strength with 6 wt.% of silica fume. A similar observation has been reported by Khater [8] who reported increasing replacement of metakaolin by silica fume up to 7 wt.% increased the strength and then decreased with further increment of silica fume. However, based on Blash & Lakshmi [9], increasing silica fume reduces mechanical strength. Nevertheless, Kouamo et al. [10] reported an increase of strength by 18.1% and 32.4% with the addition of 20wt.% and 40 wt.% of alumina into metakaolin and volcanic ash geopolymer. According to Zidi et al. [11] and Alomayri [12], the addition of 2 wt.% of nano-alumina led to a homogeneous structure.

Therefore, in this paper, the comparison between the properties of fly ash geopolymer concretes with the addition of silica fume and alumina. In previous literature, the dosage of silica fume and alumina incorporated in geopolymer were high and were added as a replacement to the aluminosilicate. In this work, the silica fume and alumina were added as an additive at low content. The dosage of silica fume and alumina was set at 2 wt.% and 4 wt.%. The physical properties, mechanical properties, and characteristics of geopolymer concrete were evaluated.

[1] CENTRE OF EXCELLENCE GEOPOLYMER AND GREEN TECHNOLOGY (CEGEOGTECH), UNIVERSITI MALAYSIA PERLIS (UNIMAP), 01000 PERLIS, MALAYSIA
[2] FACULTY OF MECHANICAL ENGINEERING TECHNOLOGY, UNIVERSITI MALAYSIA PERLIS (UNIMAP), 02600 PERLIS, MALAYSIA
[3] FACULTY OF CHEMICAL ENGINEERING TECHNOLOGY, UNIVERSITI MALAYSIA PERLIS (UNIMAP), 01000 PERLIS, MALAYSIA
[4] REACTOR TECHNOLOGY CENTER, TECHNICAL SUPPORT DIVISION, MALAYSIAN NUCLEAR AGENCY, BANGI, 43000 KAJANG, MALAYSIA
[5] DEPARTMENT OF ELECTRICAL & ELECTRONIC ENGINEERING, LEE KONG CHIAN FACULTY OF ENGINEERING & SCIENCE, UNIVERSITI TUNKU ABDUL RAHMAN, BANDAR SUNGAI LONG, 43000 KAJANG, MALAYSIA

* Coresspondence author: chengyongheah@hotmail.com

2. Methodology

2.1. Materials

The Class F fly ash used was collected from Sultan Azlan Shah Power Station, Manjung, Perak. The fly ash consists mainly of SiO_2 and Al_2O_3 based on the chemical composition analysis tabulated in Table 1. The fly ash is spherically shaped with a smooth surface (Fig. 1). The liquid sodium silicate (Na_2SiO_3, South Pacific Chemical Industries Sdn. Bhd. (SPCI), Malaysia) has a chemical composition of 60.5 wt.% H_2O, 30.1 wt.% SiO_2, 9.4 wt.% Na_2O and SiO_2/Na_2O modulus of 3.2. The sodium hydroxide (NaOH, HmbG® Chemicals) has an assay of 98.0-100.5%.

Silica fume (Sigma-Aldrich) is nanosilica with a particle size of 7 nm while alumina (Alfa Aesar) has 99% purity with a density of 3.96 g/cm^3. River sand was used as the fine aggregate and gravel was used as the coarse aggregate.

TABLE 1

Chemical composition of fly ash by XRF

Compound	SiO_2	Al_2O_3	Fe_2O_3	CaO	Others
Mass (%)	56.3	28.0	6.86	3.89	4.95

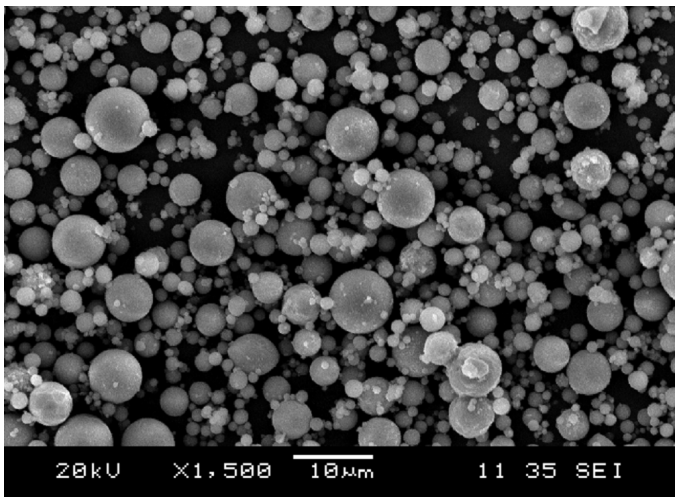

Fig. 1. SEM micrograph of fly ash

2.2. Synthesis of Geopolymer Concrete

Fly ash, river sand and gravel were dry-mixed. The content of aggregate was set as 70%. The sand/gravel ratio was fixed at 3:2. The alkali activator was then added into the dry mixture with a fly ash/alkali activator ratio of 2.0. The alkali activator consisted of the NaOH 10M solution and Na_2SiO_3 at the ratio of 2.5. Silica fume (2 wt.% and 4 wt.%) and alumina (2 wt.% and 4 wt.%) were added separately into the geopolymer concrete mixture and cast into 100 × 100 × 100 mm moulds. The fresh geopolymer concrete was cured at room temperature for 24 hours followed by curing at 60°C for another 24 hours.

2.3. Testing and Analysis

The bulk density of geopolymer concrete was obtained by measuring the mass and dimension of the concrete sample in accordance with BS EN 12390-7. Based on ASTM C642, the wet mass (M_w), dry mass (M_d) and suspended mass (M_s) were measured. The water absorption and apparent porosity were calculated based on Eq. (1) and (2).

$$\text{Water Absorption} = \frac{M_w - M_d}{M_d} \quad (1)$$

$$\text{Apparent Porosity} = \frac{M_w - M_d}{M_w - M_s} \quad (2)$$

The compressive strength test was carried out by using the universal testing machine (Shimadzu UH-1000KNI) according to ASTM C109. The concrete sample was loaded at a constant rate of 5 mm/min. Three samples were compressed to obtain the average strength value.

The morphology of geopolymer concretes was revealed using a scanning electron microscope (JEOL, JSM-6460LA). The specimen was cut section and coated with auto fine coater (JEOL JFC 1600) before analysis.

The functional group analysis of the geopolymer sample was performed using a FTIR spectrometer (Perkin Elmer RX1). The specimen was scanned from 650 cm^{-1} to 4000 cm^{-1} with a resolution of 4 cm^{-1}.

3. Result and Discussion

3.1. Bulk Density, Apparent Porosity and Water Absorption

Fig. 2 displays the bulk density, apparent porosity, and water absorption of fly ash geopolymer concretes with the addition of silica fume and alumina. The bulk density of geopolymer concrete increased with increasing silica fume content up to 2 wt.% and then decreased at 4 wt.% of silica fume. A similar observation has been reported in our previous paper [13] for fly ash geopolymer. The addition of silica fume contributed more active Si for the geopolymerization reaction. However, excess Si inhibited the dissolution of Al from fly ash and reduced the density. Whereas geopolymer concrete showed an increment in the bulk density with increasing alumina content up to 4 wt.%. Also, the incorporation of alumina imparted additional active Al for network formation before the dissolution of Al from fly ash. This accelerated the geopolymerization reaction and formed a denser microstructure [14]. The apparent porosity and water absorption result complied with the bulk density result, wherein the geopolymer concrete with higher bulk density has lower apparent porosity and water absorption.

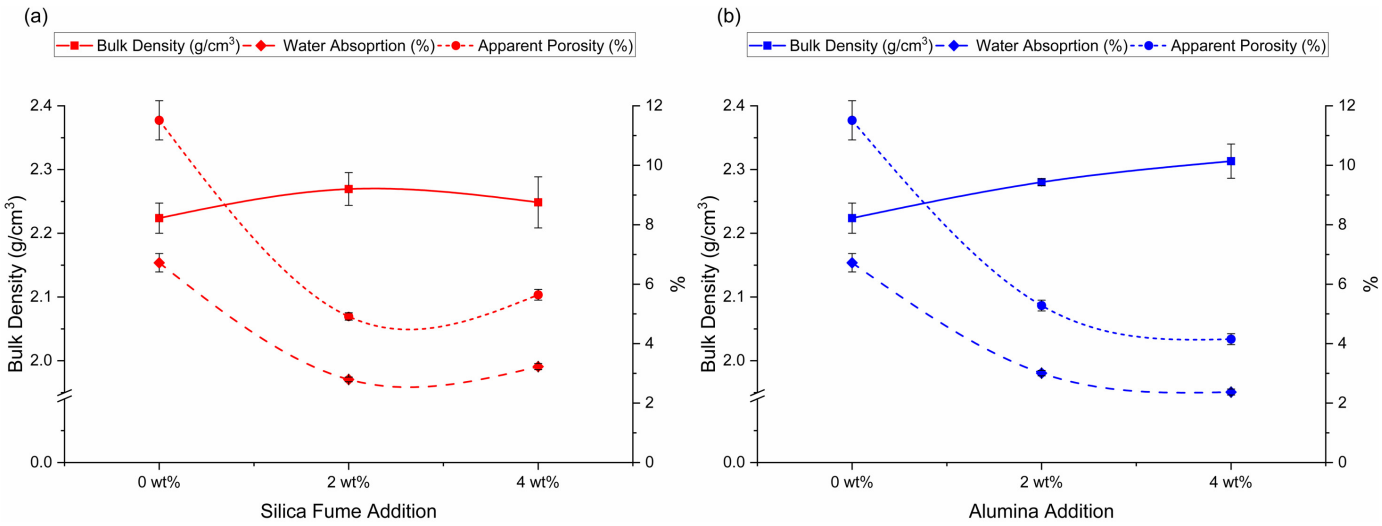

Fig. 2. Bulk density, apparent porosity, and water absorption of fly ash geopolymer concrete with the addition of (a) silica fume and (b) alumina

3.2. Compressive Strength

Fig. 3 shows the compressive strength of fly ash geopolymer concretes with the addition of silica fume and alumina. The geopolymer concrete without additive has a compressive strength of 19 MPa after 28 days of curing. The addition of 2 wt.% of silica fume increased the compressive strength to 39 MPa (increment of 105%). The compressive strength dropped to 25 MPa at 4 wt.% of silica fume. On the other hand, the compressive strength of geopolymer concrete increased with increasing alumina content. The highest compressive strength achieved was 41 MPa (increased by 115%) with 4 wt.% of alumina. The compressive strength result was consistent with the bulk density, apparent porosity, and water absorption results as shown in Fig. 2.

The geopolymer has Si-O-Al polymeric network constructed from Al^{3+} and Si^{4+} ions. Hence, when alumina and silica were added to the geopolymer mixture, they provided additional Al and Si contents to develop the geopolymer network [15,16]. However, the effect of adding alumina and silica was different based on the compressive strength result in Fig. 3. According to Garcia-Lodeiro et al. [17], Al dissolves faster than Si during the dissolution step. Thus, when adding silica in a small amount, it helped to boost the formation of geopolymer bonding. Nevertheless, the formation of a high amount of geopolymer gel at an early stage will slow down the dissolution of Al and Si from fly ash. The higher Si content restricted the aluminosilicate gel to react continuously [18]. Contrarywise, the alumina addition accelerated the dissolution of Al and Si from fly ash [10]. The increasing strength trend with increasing alumina content was also reported by Huang & Han [14].

3.3. Morphology Analysis

Fig. 4 reveals the SEM micrographs of geopolymer concretes with and without silica fume and alumina. The transformation in the morphology of geopolymer concrete was evident with the different addition of silica fume and alumina.

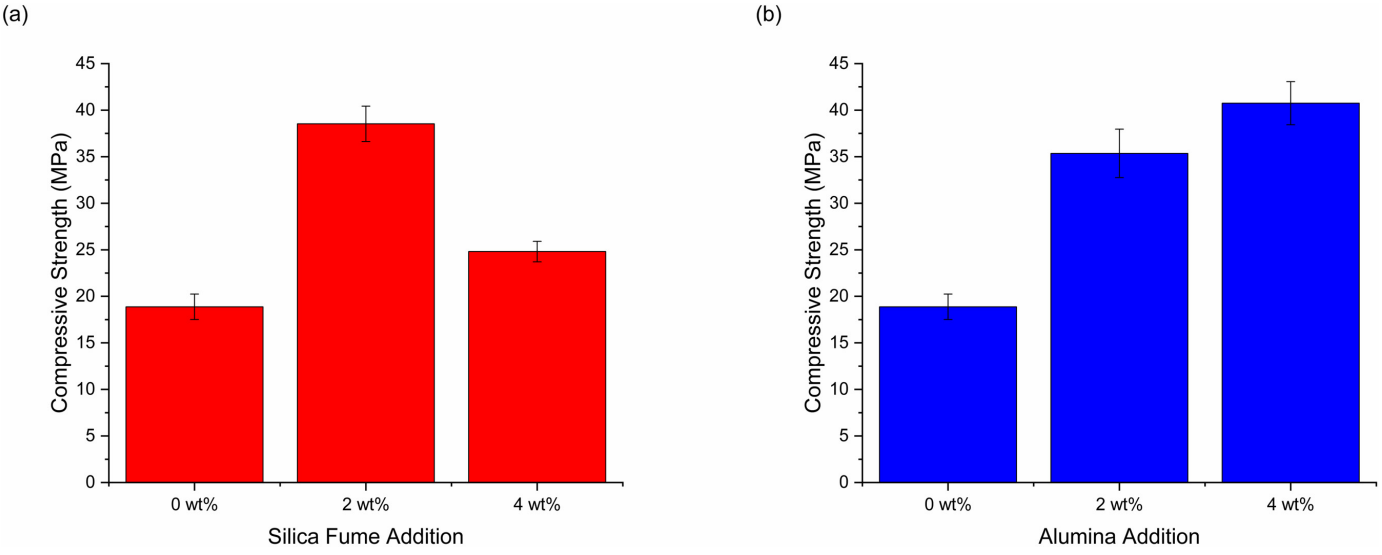

Fig. 3. Compressive strength of fly ash geopolymer concrete with the addition of (a) silica fume and (b) alumina

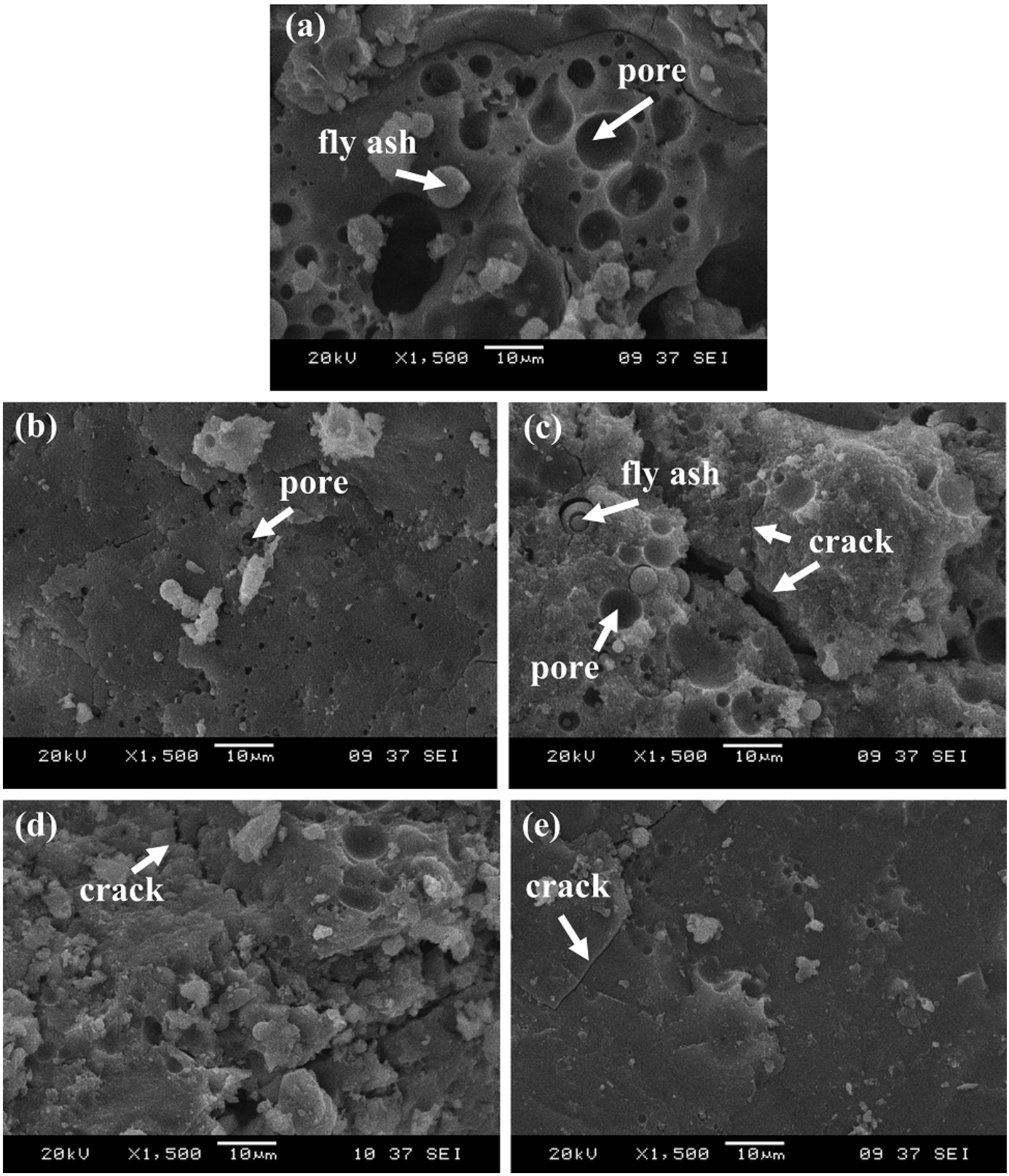

Fig. 4. SEM micrographs of fly ash geopolymer concrete (a) without additive; and with addition of (b) 2 wt.% silica fume; (c) 4 wt.% of silica fume; (d) 2 wt.% of alumina; and (e) 4 wt.% of alumina

The geopolymer sample without additive showed a relatively smooth geopolymer matrix with large pores and some remnant fly ash particles. The geopolymer sample with 2 wt.% of silica fume demonstrated a dense geopolymer matrix. The addition of silica fume promoted the formation of more geopolymer matrix with lesser pores. Based on Kang-Wei et al. [19], unreacted silica fume will fill up the pores within the binder and lower the pore distribution.

A similar microstructure was observed for the sample with 4 wt.% of alumina. Increasing alumina content boosted the ge-

opolymerization reaction and produced a compact geopolymer matrix with excellent compressive strength. The observation was also supported by Zidi et al. [11] and Alomayri [12], as aforementioned. Yet, the microstructure became loose with the presence of cracks and pores with 4 wt.% of silica fume. The presence of cracks was believed one of the factors that caused the degradation of compressive strength. The observation was in compliment with the compressive strength result as shown in Fig. 3.

3.4. Functional Group Analysis

Fig. 5 illustrates the IR spectra of fly ash and fly ash geopolymer concretes with the addition of silica fume and alumina. In general, the fly ash and geopolymers have some absorption bands in common. The absorption band at ~3600 cm^{-1}, attributed to the OH stretching vibration [20]. The band at ~1660 cm^{-1} was assigned as the H-O-H bending [21]. The stretching vibration of O-C-O can be seen at 2169-2348 cm^{-1} and ~1520 cm^{-1} [22].

The fly ash showed the main absorption band at 1028 cm^{-1}, representing the asymmetric stretching vibration of Si-O-Si and Si-O-Al [23]. This band shifted to a lower wavenumber (~980 cm^{-1}) after geopolymerization reaction due to the formation of aluminosilicate matrix [20]. It was noticed that the increasing silica fume content in geopolymer shifted the wavenumber from 984 cm^{-1} to 990 cm^{-1}. On the other hand, the wavenumber reduced from 984 cm^{-1} to 979 cm^{-1} with increasing alumina. This implied that the geopolymer matrix with silica fume was rich in Si while those with alumina were rich in Al. Based on Nikolov et al. [24], incorporation of Al^{3+} ion into $(SiO_4)^{4-}$ ion reduced the wavenumber. Nevertheless, no additional absorption band was observed due to the incorporation of silica fume and alumina.

4. Conclusion

The paper presented a comparative study of the effect of adding silica fume and alumina on the properties of fly ash geopolymer concrete. Results showed that the addition of 2 wt.% of silica fume (39 MPa) and 4 wt.% of alumina (41 MPa) produced the highest compressive strength and bulk density while the lowest porosity and water absorption. As proven by the SEM images, the geopolymer concrete with 2 wt.% of silica fume and 4 wt.% of alumina demonstrated a smooth and compact geopolymer matrix. The incorporation of both silica fume and alumina induced supplementary Si and Al at the early stage to form the geopolymer network. In spite, the dosage of silica fume tolerated by the geopolymer system was low (2 wt.% of silica fume) because it will impede the dissolution of Al and Si from aluminosilicate (that is, fly ash) and subsequently affect the geopolymerization reaction. In contrast, the addition of alumina will help to enhance the dissolution of fly ash.

Acknowledgement

The authors wish to gratefully acknowledge the facility support from Faculty of Mechanical Engineering Technology and Faculty of Chemical Engineering Technology, Universiti Malaysia Perlis, Malaysia.

REFERENCES

[1] E.A. Azimi, M.M.A.B. Abdullah, L.Y. Ming, H.C. Yong, K. Hussin, I.H. Aziz, Rev. Adv. Mater. Sci. **44**, 273-285 (2016).

[2] Z. Hu, M. Wyrzykowski, P. Lura, Cem. Concr. Res. **129**, 105971 (2020). DOI: https://doi.org/10.1016/j.cemconres.2020.105971

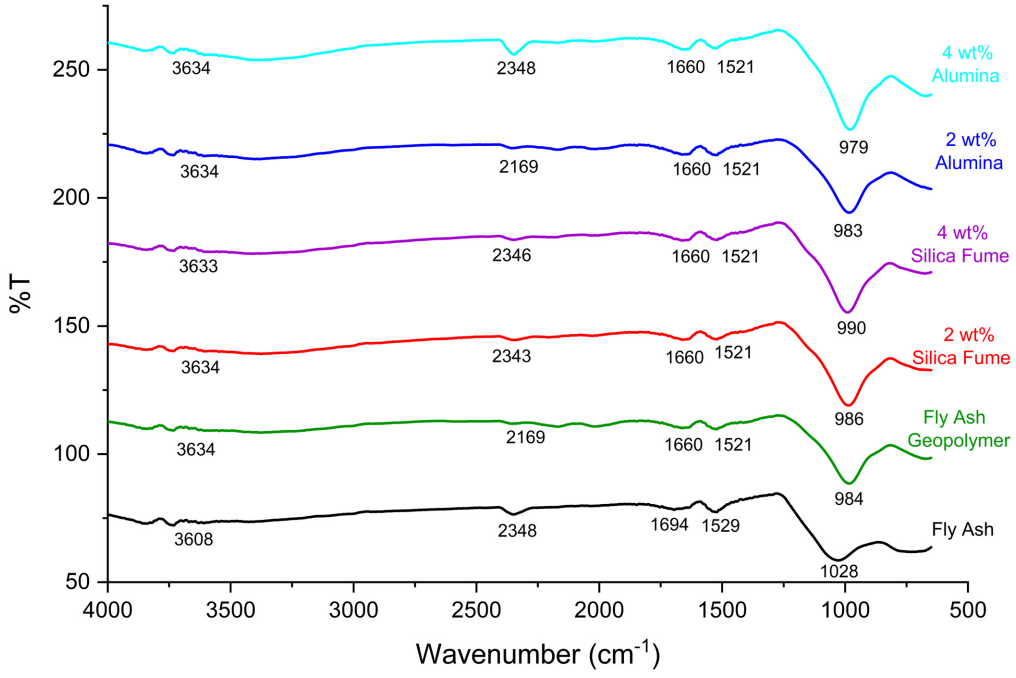

Fig. 5. IR spectra of fly ash and fly ash geopolymer concrete with silica fume and alumina addition

[3] C. Kuenzel, N. Ranjbar, Resour. Conserv. Recycl. **150**, 104421 (2019). DOI: https://doi.org/10.1016/j.resconrec.2019.104421

[4] K. Zulkifly, H.C. Yong, M.M.A.B. Abdullah, L.Y. Ming, D. Panias, K. Sakkas, in IOP Conference Series: Materials Science and Engineering **209**, 012085 (2017). DOI: https://doi.org/10.1088/1757-899x/209/1/012085

[5] Y. Liu, C. Shi, Z. Zhang, N. Li, D. Shi, Cem. Concr. Compos. **112**, 103665 (2020). DOI: https://doi.org/10.1016/j.cemconcomp.2020.103665

[6] F.N. Okoye, S. Prakash, N.B. Singh, J. Clean. Prod. **149**, 1062-1067 (2017). DOI: https://doi.org/10.1016/j.jclepro.2017.02.176

[7] A. Nmiri, M. Duc, N. Hamdi, O. Yazoghli-Marzouk, E. Srasra, Int. J. Miner. Metall. Mater. **26**, 555-564 (2019). DOI: https://doi.org/10.1007/s12613-019-1764-2

[8] H.M. Khater, Int. J. Adv. Struct. Eng. **5**, 12 (2013). DOI: https://doi.org/10.1186/2008-6695-5-12

[9] A.M.A. Blash, T.V.S. . Lakshmi, Int. J. Sci. Res. **5**, 319-323 (2016). https://www.ijsr.net/search_index_results_paperid.php?id=ART20162136

[10] H.T. Kouamo, A. Elimbi, J. Mbey, C.J.N. Sabouang, D. Njopwouo, Construct. Build. Mater. **35**, 960-969 (2012). DOI: https://doi.org/10.1016/j.conbuildmat.2012.04.023

[11] Z. Zidi, M. Ltifi, Z.B. Ayadi, L.E. Mir, J. Asian Ceram. Soc. **7**, 524-535 (2019). DOI: https://doi.org/10.1080/21870764.2019.1676498

[12] T. Alomayri, J. Build. Eng. **25**, 100788 (2019). DOI: https://doi.org/10.1016/j.jobe.2019.100788

[13] O. Huey Li, L. Yun-Ming, H. Cheng-Yong, R. Bayuaji, M.M.A.B. Abdullah, F. Kai-Loong, T. Soo-Jin, N. Hui-Teng, M. Nabiałek, B. Jez, N. Yong-Sing, Magnetochemistry **7** (1), (2021). DOI: https://doi.org/10.3390/magnetochemistry7010009

[14] Y. Huang, M. Han, J. Hazard. Mater. **193**, 90-94 (2011). DOI: https://doi.org/10.1016/j.jhazmat.2011.07.029

[15] R. Cioffi, L. Maffucci, L. Santoro, Resour. Conserv. Recycl. **40**, 27-38 (2003). DOI: https://doi.org/10.1016/S0921-3449(03)00023-5

[16] J. Davidovits, J. Therm. Anal. **37**, 1633-1656 (1991). DOI: https://doi.org/10.1007/bf01912193

[17] I. Garcia-Lodeiro, A. Palomo, A. Fernández-Jiménez, 2 – An overview of the chemistry of alkali-activated cement-based binders, in: F. Pacheco-Torgal, J.A. Labrincha, C. Leonelli (Eds), Handbook of Alkali-Activated Cements, Mortars and Concretes 2015, Woodhead Publishing (2015). DOI: https://doi.org/10.1533/9781782422884.1.19

[18] P. Posi, C. Ridtirud, C. Ekvong, D. Chammanee, K. Janthowong, P. Chindaprasirt, Construct. Build. Mater. **94**, 408-413 (2015). DOI: https://doi.org/10.1016/j.conbuildmat.2015.07.080

[19] L. Kang-Wei, L. Kae-Long, C. Ta-Wui, C. Yu-Min, L. Ju-Ying, Construct. Build. Mater. **143**, 455-463 (2017). DOI: https://doi.org/10.1016/j.conbuildmat.2017.03.152

[20] J.K. Prusty, B. Pradhan, Construct. Build. Mater. **241**, 118049 (2020). DOI: https://doi.org/10.1016/j.conbuildmat.2020.118049

[21] G. Ishwarya, B. Singh, S. Deshwal, S.K. Bhattacharyya, Cem. Concr. Compos. **97**, 226-238 (2019). DOI: https://doi.org/10.1016/j.cemconcomp.2018.12.007

[22] B. Aissa, L. Long-yuan, A.B.A. Mohd Mustafa, B. Quoc-Bao, Construct. Build. Mater. **210**, 198-209 (2019). DOI: https://doi.org/10.1016/j.conbuildmat.2019.03.202

[23] I. Perná, M. Šupová, T. Hanzlíček, A. Špaldoňová, Construct. Build. Mater. **228**, 116765 (2019). DOI: https://doi.org/10.1016/j.conbuildmat.2019.116765

[24] A. Nikolov, H. Nugteren, I. Rostovsky, Construct. Build. Mater. **243**, 118257 (2020). DOI: https://doi.org/10.1016/j.conbuildmat.2020.118257